Int. J. Electron. Commun. (AEÜ) 66 (2012) 189–194

Contents lists available at ScienceDirect

International Journal of Electronics and Communications (AEÜ)

journal homepage: www.elsevier.de/aeue

A compact CPW fed slot antenna for ultra wide band applications

V.A. Shameena [b], S. Mridula [a], Anju Pradeep [a], Sarah Jacob [b], A.O. Lindo [b], P. Mohanan [b,*]

[a] School of Engineering, CUSAT, India
[b] Centre for Research in Electromagnetics and Antennas (CREMA), Department of Electronics, Cochin University of Science and Technology, Cochin 22, Kerala, India

ARTICLE INFO

Article history:
Received 28 September 2010
Accepted 20 March 2011

Keywords:
CPW fed antennas
Uniplanar antennas
UWB antennas
Time domain analysis

ABSTRACT

A printed compact coplanar waveguide fed triangular slot antenna for ultra wide band (UWB) communication systems is presented. The antenna comprises of a triangular slot loaded ground plane with a T shaped strip radiator to enhance the bandwidth and radiation. This compact antenna has a dimension of 26 mm × 26 mm when printed on a substrate of dielectric constant 4.4 and thickness 1.6 mm. Design equations are implemented and validated for different substrates. The pulse distortion is insignificant and is verified by the measured antenna performance with high signal fidelity and virtually steady group delay. The simulation and experiment reveal that the proposed antenna exhibits good impedance match, stable radiation patterns and constant gain and group delay over the entire operating band.

1. Introduction

Ultra-wide band (UWB) technology is one of the most promising solutions for future communication systems due to high data rate and excellent immunity to multi-path interference. The allocation of the frequency band from 3.1 to 10.6 GHz by FCC [1] for ultra wide band radio applications has presented an opportunity and challenge for antenna designers. As the key component of UWB system, the feasible UWB antenna design faces many challenges including the impedance match with good radiation stability in the entire band, compact antenna size and low manufacturing cost for consumer electronics applications.

For applications in portable systems, compact, radiation efficient and printed antennas are desired. Slot antennas satisfy these requirements where wide bandwidth can be obtained by different techniques. Owing to a balanced structure, CPW fed antennas are very good candidates since the feed lines and the slots are on the same side of the substrate. The antennas discussed in Ref. [2] use a large slot for bandwidth enhancement and L or T shapes for size reduction. A CPW fed tapered ring slot antenna which can achieve a relatively large bandwidth is introduced in Ref. [3]. The wide band slot antenna [4] uses a large aperture and a modified microstrip feed to create multiple resonances. In another technique, a rotated slot is proposed [5] wherein two modes of close resonances are excited by a microstrip feed line. A tapered slot feeding structure is used to transform the guided waves to free space waves in Ref. [6]. In Ref. [7], a microstrip fed triangular slot antenna with a double T shaped tuning stub is introduced. The double T shaped stub is fully positioned within the slot region on the opposite side of the triangular slot. But the antenna has large dimension of 55 mm × 65 mm with limited bandwidth of 3.3 GHz.

In this paper, the triangular slot antenna [7] is modified for enhanced bandwidth and radiation characteristics to cater to the modern communication systems. The antenna comprises of a triangular slot fed by a CPW feed terminated with a T shaped structure. Even though multiresonant antennas [8] offer a wide impedance bandwidth, they widen a narrow pulse in the time domain. It is the multiple reflections within the antenna that results in the ringing of the pulse. Such detrimental effects on the transmitted pulse can be minimized if the higher order modes excited within the operating band are avoided. The proposed antenna introduces only three resonances within the operating band. Also this geometry is very compact compared to earlier designs where ultra wide bandwidth was realized using a rectangular slot [9]. The 2:1 VSWR bandwidth of this antenna is from 3.1 to 11.1 GHz which is wide enough to cover the FCC approved UWB. The antenna exhibits good impedance match, stable radiation patterns and constant group delay over the entire UWB band. Moreover, the exciting T structure has simple geometry with less parameters, releasing the computation load in the optimization process.

2. Antenna geometry, results and discussions

The geometry of the proposed antenna is shown in Fig. 1. The antenna consists of an isosceles triangular slot of side L_2 and base $2L_3 + W + 2G$ etched on a square substrate of size $L_1 \times L_1$ having dielectric constant $\epsilon_r = 4.4$, loss tangent tan $\delta = 0.02$ and thickness $h = 1.6$ mm. The strip width (W) and gap (G) of the coplanar waveguide (CPW) feed are derived using standard design equations for 50 Ω input impedance [10]. A rectangle of length L and width W is

* Corresponding author. Tel.: +91 484 2576418; fax: +91 484 2575800.
E-mail address: drmohan@gmail.com (P. Mohanan).

1434-8411/$ – see front matter © 2011 Elsevier GmbH. All rights reserved.
doi:10.1016/j.aeue.2011.03.015

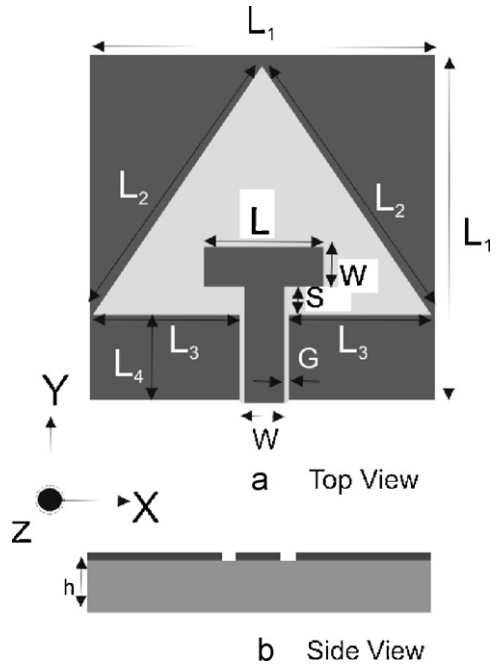

Fig. 1. Geometry of the proposed antenna (L_1 = 26 mm, L_2 = 22.65 mm, L_3 = 10.85 mm, L_4 = 7 mm, S = 2 mm, W = 3 mm, h = 1.6 mm, ϵ_r = 4.4 and G = 0.35 mm). (a) Top view. (b) Side view.

connected to the end of the CPW feed line to form a T shaped structure. The spacing between the rectangle and the edge of the ground plane is S. First two resonances are produced by the triangular slot. The rectangular stub acts as a matching element for the first two resonances and produces the third resonance.

The simulated (ANSOFT HFSS) and the experimental (HP8510C Network analyzer) reflection characteristics shows good agreement as shown in Fig. 2. The antenna has a 2:1 VSWR bandwidth from 3.1 to 11.1 GHz which is wide enough to cover the UWB criteria of FCC. Also it is clear that wide bandwidth is obtained by merging three resonances around 3.38, 4.8 and 9.5 GHz.

In order to study the effect of strip length L on the return loss characteristics, a thorough parametric analysis has been performed. Fig. 3 shows the variation of reflection characteristics and input impedance for different strip lengths L. It is observed that without the strip (L = 3), there are only two poorly matched

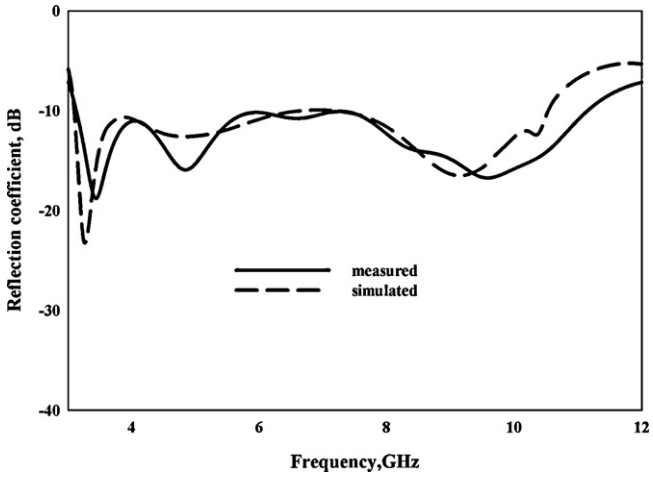

Fig. 2. Measured and simulated return losses of the antenna. (L_1 = 26 mm, L_2 = 22.65 mm, L_3 = 10.85 mm, L_4 = 7 mm, S = 2 mm, W = 3 mm, h = 1.6 mm, ϵ_r = 4.4 and G = 0.35 mm)

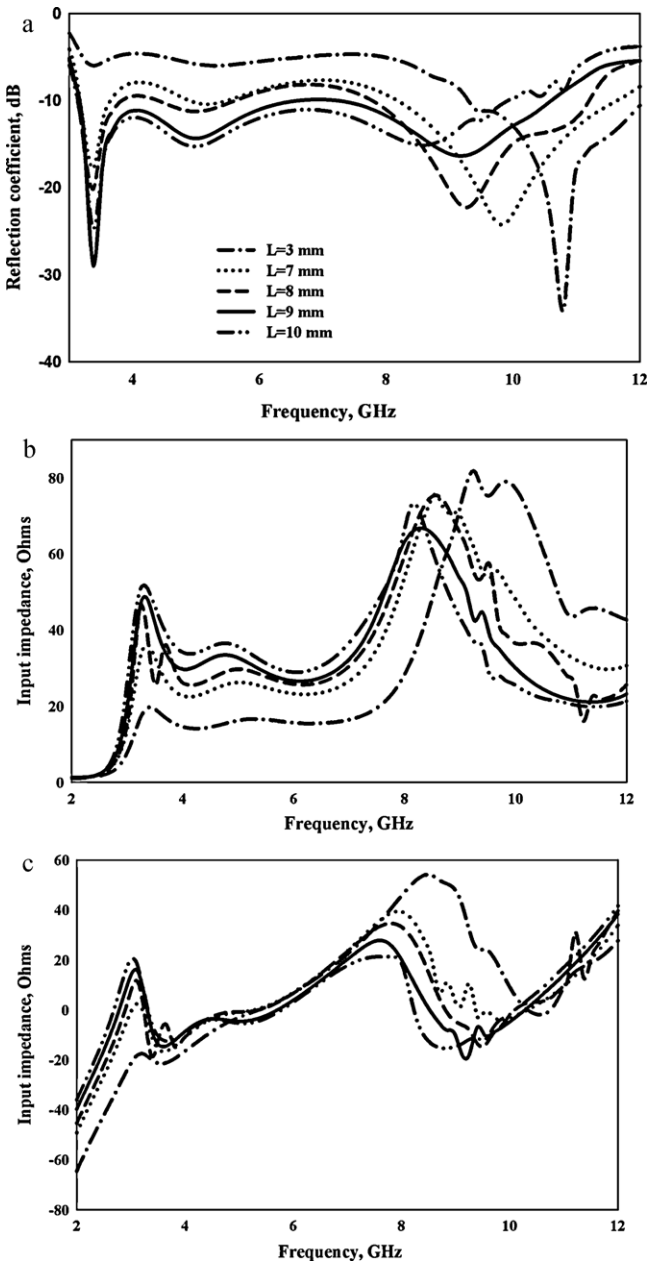

Fig. 3. Return losses and impedances of the antenna for different L. (a) Return loss. (b) Real part. (c) Imaginary part.

resonances within the UWB frequency range. As L increases, matching corresponding to the first and second resonances increases. The strip produces a third resonance and at the optimum strip length, three resonances merge together to form UWB frequency response. It can also be seen that without the strip, the antenna has very low input impedance and is highly capacitive. Increase in L improves the input impedance corresponding to the first and second resonances. Also the imaginary part is shifted towards the inductive side.

Another important factor regarding the impedance matching is the gap distance S, which adjusts the coupling between the radiating element and the ground plane. Variation of return losses and input impedances of the antenna for different gap distances are shown in Fig. 4. For S = 1 mm, matching is very poor for the first two resonances and real part of impedance is low (24 Ω), but impedance improves with increase in S and a value of 50 Ω is achieved at

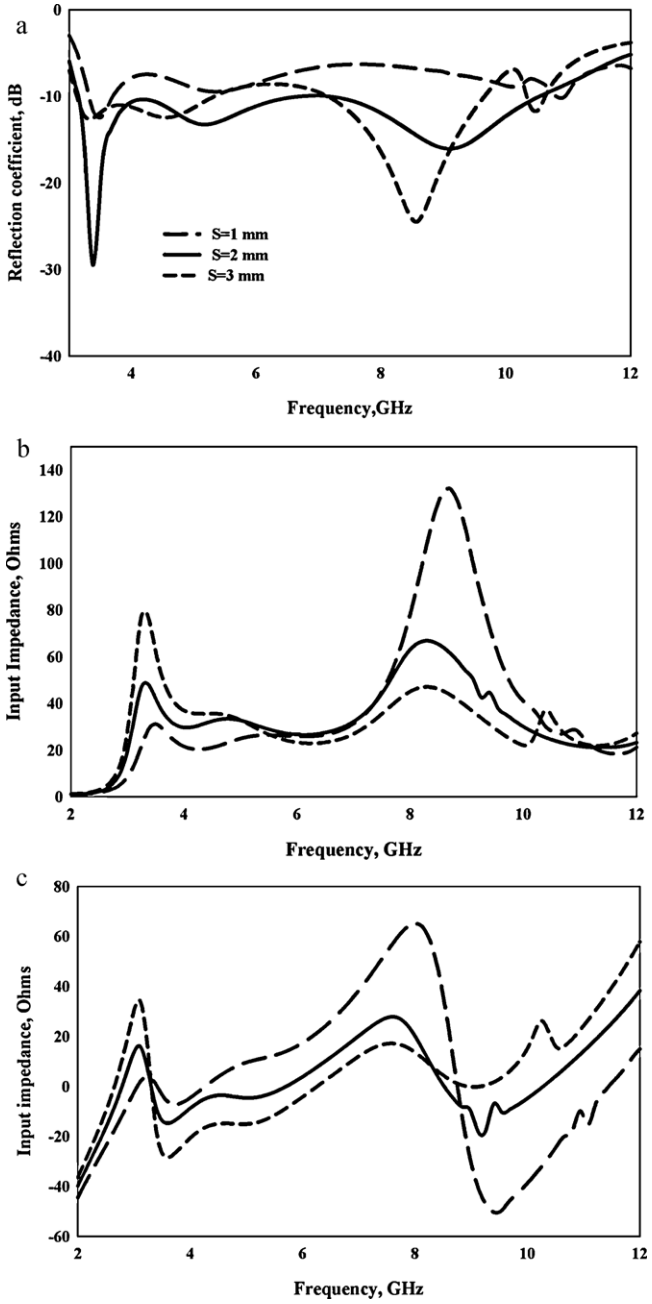

Fig. 4. Return losses and impedances of the antenna for different *S*. (a) Return loss. (b) Real part. (c) Imaginary part.

S = 2 mm. Also increase in *S* increases the inductive reactance. When *S* = 3 mm, real part of impedance is further increased and the imaginary part is shifted towards inductive side.

The current pattern of the antenna at the resonant frequencies are analyzed using HFSS. Fig. 5 shows current distribution of the antenna for three resonances. From the figures it is clear that both first and second resonances are produced by the symmetrical path ABC and DEC. First resonance is due to λ variation along the perimeter of the perpendicular slot. But the second resonance is due to 1.5λ variation along the same path. Third resonance corresponds to a λ/4 variation along the path FG.

Based on the parametric observations and current distribution aforementioned, a design procedure for the triangular slot antenna can be framed as explained in this section. Since we are interested in the ultra wide bandwidth, centre frequency of operating band is taken in to account while deriving the design equations. The criteria for designing the antenna is as follows:

Table 1
Antenna description.

	Ant.1	Ant.2	Ant.3	Ant.4
Laminate	Rogers 5880	FR4 Epoxy	Rogers RO3006	ROGERS 6010LM
h (mm)	1.57	1.6	1.28	0.635
ϵ_r	2.2	4.4	6.15	10.2
ϵ_{re}	1.6	2.7	3.575	5.6
W (mm)	4	3	2.58	2.05
G (mm)	0.17	0.35	0.45	0.5

Table 2
Computed geometric parameters of the antennas.

Parameter (mm)	Ant.1	Ant.2	Ant.3	Ant.4
L_1	33.8	26	22.5	18
L_2	29.47	22.6	19.65	15.6
L_3	14.1	10.85	9.4	9
L_4	9.11	7	6	4.85
S	2.6	2	1.735	1.36
L	11.71	9	7.8	6.22

(1) Design a 50 Ω CPW line on a substrate with permittivity ϵ_r. Calculate ϵ_{reff} using $\epsilon_{reff} = (\epsilon_r + 1)/2$ where ϵ_{reff} is the effective permittivity of the substrate.
(2) Ground plane plays a major role in determining the first and second resonances. The dimensions of the ground plane are calculated as follows:

$$L_1 = (\lambda_c) \quad (1)$$

$$L_4 = (0.27 * \lambda_c) \quad (2)$$

where λ_c is the wavelength corresponding to centre frequency of the operating band.
(3) Sides of the triangle L_2 and L_3 are calculated using

$$L_2 = (0.87 * \lambda_c) \quad (3)$$

and

$$L_3 = (0.417 * \lambda_c). \quad (4)$$

(4) Length of the rectangular stub L and the gap between stub and ground plane separation S are calculated using

$$S = 0.076 * \lambda_c \quad (5)$$

and

$$L = 0.346 * \lambda_c \quad (6)$$

.

In order to justify the design equations, the antenna parameters are computed for different substrates (Table 1) and are tabulated in Table 2.

Fig. 6 shows the return losses of different antennas as given in Table 2. In all the cases antenna is operating in the UWB region.

Fig. 7 shows the measured radiation patterns of the antenna at frequencies 3.4, 4.8 and 9.6 and 10.6 GHz, respectively. The antenna is linearly polarized along Y direction with better cross polar isolation in the entire band of operation.

The measured gain and the radiation efficiency of the antenna are shown in Fig. 8. In the entire band, the antenna offers good gain with a peak gain of 5.5 dBi at 11 GHz. Efficiency is measured using Wheeler cap method. Average efficiency of the antenna is found to be 72%.

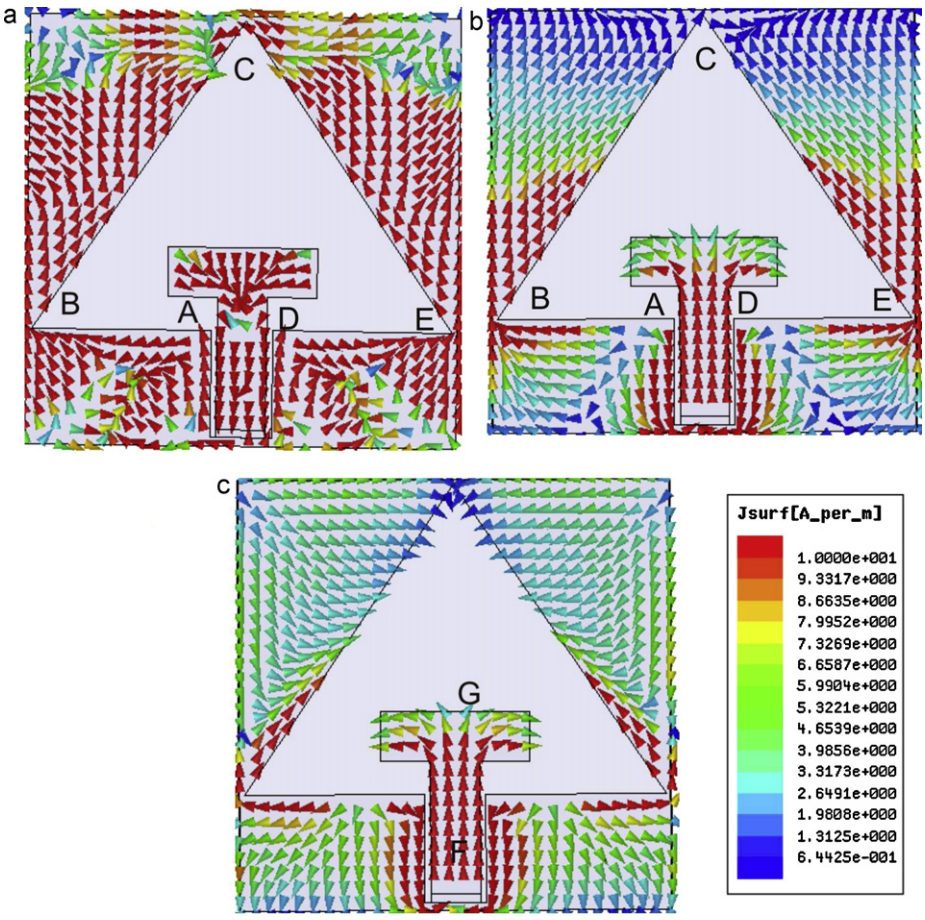

Fig. 5. Current distribution of the antenna at resonant frequencies. (a) 3.38 GHz; (b) 4.78 GHz and (c) 9.6 GHz.

3. Time domain antenna analysis

As shown in the previous section, the proposed antenna has very wide bandwidth. However, having a wide frequency domain response does not necessarily ensure excellent pulse handing capability. To explore this the time domain responses of the antennas are explored. Therefore, transfer characteristics of the two proposed identical antennas in free space are studied [11]. The group delay measurements were performed using two identical prototype antennas. As shown in Fig. 9, the measured group delay remains almost constant with variation less than 2 nanosecond for the face to face and side by side orientations. This indicates a good time domain performance of the antenna.

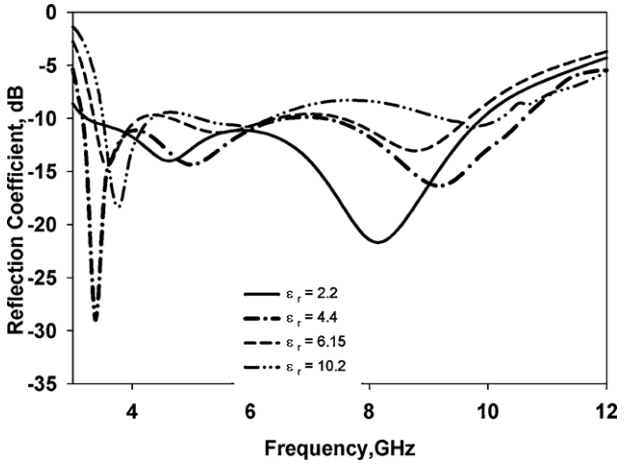

Fig. 6. Reflection coefficient of the antenna with computed geometric parameter for different substrates.

Transient response of the antenna is studied by modeling the antenna by its transfer function. For this, the transmission coefficient S_{21} is measured using HP8510C Network analyzer in the frequency domain for the face-to-face and side-by-side orientations placing the antennas at a distance $R = 10$ cm. The transfer function is computed from this as

$$H(w) = \sqrt{\frac{2\pi R C S_{21}(w) e^{jwR/C}}{jw}} \tag{7}$$

where c is the free space velocity and R is the distance between the two antennas. The measured transfer function is first transformed to time domain $[H(t)]$ by performing the inverse Fourier transform. Incident wave arriving at the receiving antenna is assumed to be the fourth derivative of a Rayleigh function given by

$$S_t(t) = \frac{16x^4 - 48x^2 + 120}{\sqrt{2\pi}} \text{ V/m.} \tag{8}$$

The output waveform at the receiving antenna terminal can therefore be expressed by

$$S_r(t) = S_t(t) \otimes H(t) \text{ V/m.} \tag{9}$$

The input and received wave forms for the face-to-face and side-by-side orientations of the antenna are shown in Fig. 10. It is evident that the received pulses are almost identical.

In UWB systems it is very important to characterize the transient behavior of the radio propagation channel, specifically for impulse radio systems. Pulse fidelity involves the autocorrelation of two

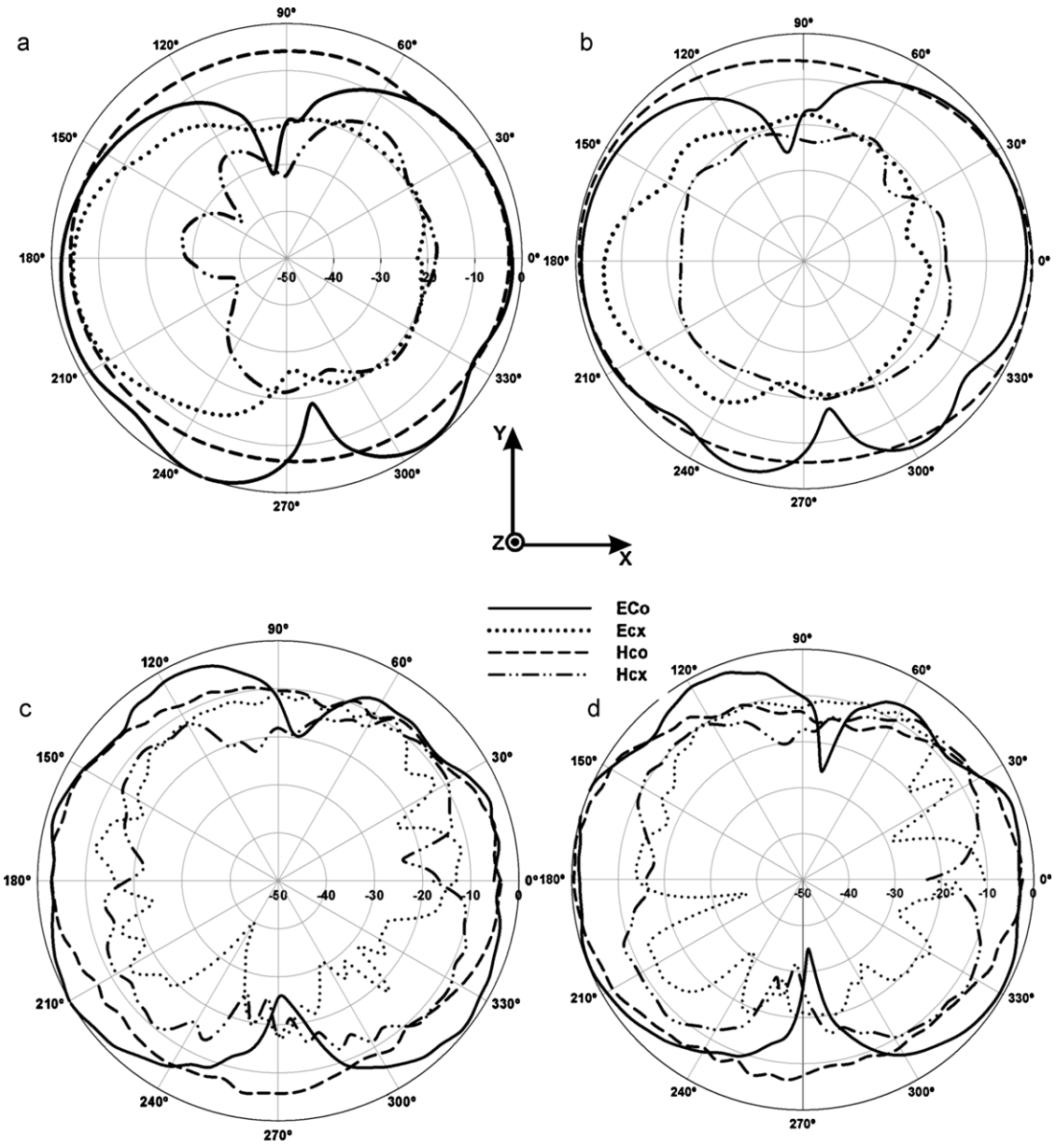

Fig. 7. Radiation patterns of the antenna at (a) 3.4 GHz; (b) 4.8 GHz; (c) 9.6 GHz and (d) 10.6 GHz.

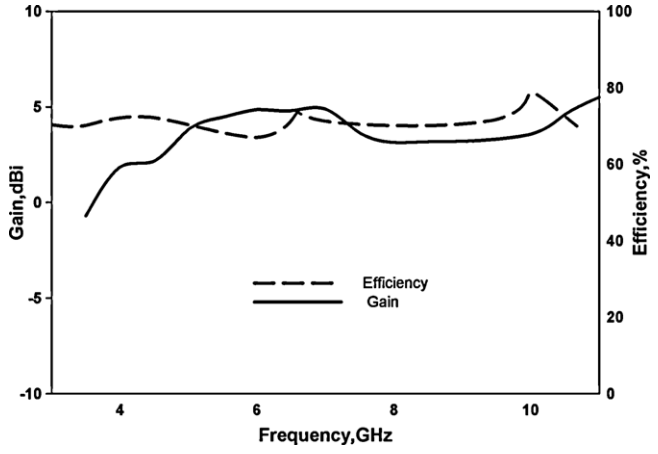

Fig. 8. Measured gain and efficiency of the antenna.

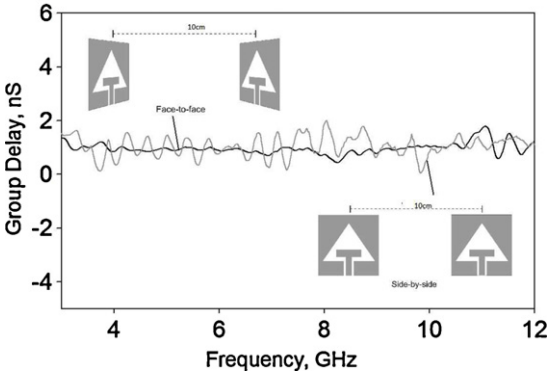

Fig. 9. Measured group delay of the antenna.

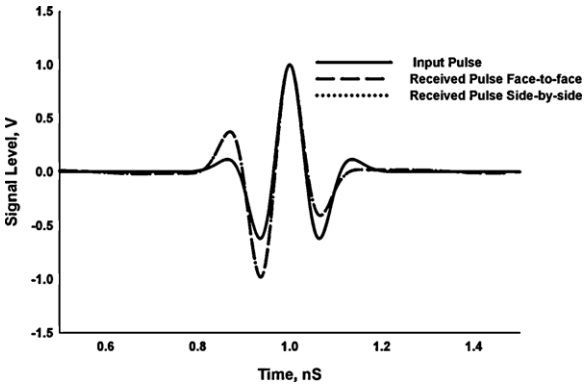

Fig. 10. Normalized input and received pulses.

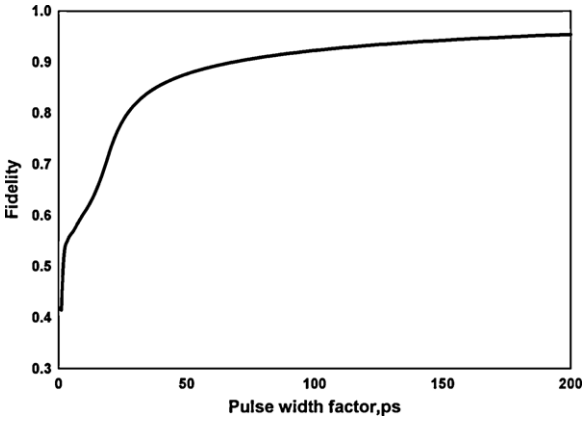

Fig. 11. Fidelity factor between transmitted and received signal for different pulse width factor.

different time domain waveforms and compares the shape of the pulses disregarding the amplitude and the time delay. A low fidelity between transmitted and received pulse means that the distortion of the received pulses is high and hence loss of system information is high [12].

$$F = \frac{\int_{-\infty}^{\infty} S_t(t)S_r(t-\tau)dt}{\sqrt{\int_{-\infty}^{\infty}|S_t(t)|^2dt\int_{-\infty}^{\infty}|S_r(t)|^2dt}} \quad (10)$$

where $s_t(t)$ is the source pulse and $s_r(t)$ is the received signal. Using the above equation, the fidelity factor between transmitted and received signals in Tx/Rx setups between two identical antennas in face to face orientation are calculated for the above mentioned fourth order Rayleigh pulse and is shown in Fig. 11. It is clear from the figure that fidelity factor can be greater than 0.9 from $\tau = 50$ ps, where τ is the pulse width fidelity factor. These values for the fidelity factor show that the antenna imposes negligible effects on the transmitted pulses.

According to FCC regulations, UWB systems must comply with stringent EIRP limits in the frequency band of operation. EIRP is the amount of power that would have to be emitted by an isotropic antenna to produce the peak power density of the antenna under test. To obtain EIRP, we use similar transmit and receive antennas and total frequency response of the system $H(w)$ is calculated.

$$EIRP = P_T(f)4\pi Rf/c\sqrt{H(w)}. \quad (11)$$

where $P_T(f)$ is the power of transmitted pulse. Fig. 12 shows the measured EIRP emission level of the antenna excited with a fourth order Rayleigh pulse with pulse width factor $\tau = 50$ ps as the excitation signal. As it is clear from the figure, EIRP of the antenna satisfies the FCC masks for the entire UWB band.

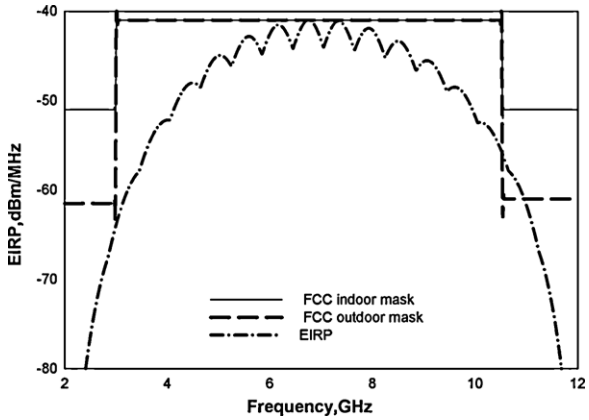

Fig. 12. EIRP emission level of the antenna for the fourth order Rayleigh pulse.

4. Conclusion

A simple compact UWB slot antenna is implemented. Broad impedance bandwidth, stable radiation patterns and constant gain are the main attractions of this antenna. Also the extensive investigations were carried out to extract the time domain behavior of the antenna. Fidelity of the antenna reveal that this antenna introduces limited distortion to baseband signals. It therefore substantiates the applicability of the proposed antenna in UWB radios. Also the EIRP of the antenna satisfies the FCC masks for the entire UWB band. The antenna can be easily fabricated on any commercially available substrates using the present design guidelines. All these features make the proposed antenna a potential candidate for emerging UWB applications.

Acknowledgements

The authors would like to acknowledge University grants commission (UGC), Department of Science and Technology (DST), Govt. of India for providing financial support.

References

[1] Siwiak K, McKeown D, pp. 97–111 Ultra wideband radio technology; 2005.
[2] Latif SI, Shafai L, Sharma SK. Bandwidth enhancement and size reduction of microstrip slot antennas. IEEE Trans Antennas Propag 2005;53:994–1003.
[3] Ma TG, Tseng CH. An ultra wide band coplanar waveguide-fed tapered ring slot antenna. IEEE Trans Antennas Propag 2006;54:1105–11.
[4] Behdad N, Sarabandi K. A multiresonant single element wide-band slot antenna. IEEE Trans Antennas Propag 2005;53:994–1003.
[5] Jan JY, Su JW. Band width enhancement of a printed wide slot antenna with a rotated slot. IEEE Trans Antennas Propag 2005;53:2111–4.
[6] Ma TG, Jeng SK. Planar miniature tapered slot fed annular slot antennas for ultra wide band radios. IEEE Trans Antennas Propag 2005;53:1194–202.
[7] JoongHan Yoon. Triangular slot antenna with a double T shaped tuning stub for wide band operation. Microw Opt Technol Lett 2007;49:2123–8.
[8] Ma TG, Jeng SK. A printed dipole antenna with tapered slot for ultra wide band applications. IEEE Trans Antennas Propag 2005;53:3833–6.
[9] Lin YC, Hung KJ. Compact ultrawideband rectangular aperture antenna and band-notched designs. IEEE Trans Antennas Propag 2006;54:3075–81.
[10] Garg R, Bhartia P, Bahl I, Ittipiboon A. Microstrip antenna design handbook. Norwood, MA: Artech House; 2001.
[11] Duroc Y, Ghiotto A, Vuong TP, Tedjini S. UWB antennas: systems with transfer function and impulse response. IEEE Trans Antennas Propag 2007;55:1449–51.
[12] Mehdipour A, Mohammadpour-Aghdam K, Faraji-Dana R. Complete dispersion analysis of vivaldi antenna for ultra wideband applications. Prog Electromagn Res PIER 2007:77.